International Journal of Medical, Medicine and Health Sciences
ISSN: 2517-9969
Vol:8, No:10, 2014

Radiobiological Model in Radiotherapy Planning for Prostate Cancer Treatment

Pradip Deb

***Abstract*—**Quantitative radiobiological models can be used to assess the optimum clinical outcome from sophisticated therapeutic modalities by calculating tumor control probability (TCP) and normal tissue complication probability (NTCP). In this study two 3D-CRT and an IMRT treatment plans were developed with an initial prescription dose of 60 Gy in 2 Gy/fraction to prostate. Sensitivity of TCP and Complication free tumor control probability (P+) to the different values of α/β ratio was investigated for various prescription doses planned to be delivered in either a fixed number of fractions (I) or in a fixed dose per fraction (II) in each of the three different treatment plans. High dose/fraction and high α/β value result in comparatively smaller P+ and IMRT plans resulted in the highest P+, mainly due to the decrease in NTCP. If α/β is lower than expected, better tumor control can be achieved by increasing dose/fraction but decreasing the number of fractions.

***Keywords*—**Linear Quadratic Model, TCP, NTCP, α/β ratio

I. Introduction

ACCORDING to the report from the International Agency for Research on Cancer (IARC), global cancer rates will increase 50% by the year 2020. More than 25% people in modern industrial countries are 'destined' to get cancer [1]. To reduce the suffering and death due to cancer is now one of the biggest challenges ever. Continuous research and technical developments give us hope and confidence about winning the battle against cancer. Radiotherapy has been a major weapon in this battle for a long time. About 60% of cancer patients receive radiotherapy as part of their disease management [2]. Three Dimensional Conformal radiation therapy (3D-CRT) and Intensity Modulated Radiation Therapy (IMRT) are being used successfully for both the palliative and curative treatments of cancer.

Prostate cancer is potentially curable if detected and treated in its early stage. There are several treatment options available for prostate cancer [3]. These treatment options vary according to the stage of the cancer and other medical conditions. Radiotherapy and surgery are the two main options used to eliminate the primary tumor [4]. Radiation therapy uses high-energy beam of radiations to kill cancer cells. At primary stage of the prostate cancer radiation is effectively used to eliminate the cancer cells. But if the cancer is in more advanced stage, radiation is primarily used to reduce the size of the tumor by partially killing the tumor cells and thus provide palliative treatment. For treatment purposes two types of radiation therapy are mainly used, (i) external beam radiation therapy and (ii) internal radiation - brachytherapy. In recent years external beam radiation therapies are being widely used for the treatment of prostate cancer. Modern development of engineering and computer technologies has opened the door of opportunities to use conformal three dimensional external radiotherapy including intensity modulated radiotherapy to treat prostate cancer [5]-[9].

The main goal of curative radiation therapy is to deliver a dose of radiation high enough to kill tumor cells at a sufficiently high probability level to control the tumor while at the same time minimizing the radiation dose to the surrounding normal tissues. Thus the normal tissue damage can be kept at a minimum level. This core aim of radiating tissues of a particular tumor gives the idea of 'conformal' radiation therapy. From this concept of irradiation technique, 3D-CRT can be defined as the process of designing external radiation beams which are able to exclusively irradiate tumor sites sparing normal tissue cells [10], [11].

It is not easy to reach the 'goal' in external beam radiotherapy as radiation beams often traverse the normal tissues adjacent to the target tumor. Thus the normal tissue complications arise. As a result the tumor control becomes difficult. The major problems in obtaining the maximum therapeutic advantage from conventional radiotherapy are due to the uncertainties of tumor volume, lack of knowledge about the structure of the normal tissues and the limitations of dose delivery systems. The usual approach to compensate this limitations is to use a large safely margin around the tumor volume to reduce the normal tissue complications. By this way, the normal tissue complications can be kept lower, but effective tumor controls cannot be obtained. So, better localizations are necessary for the tumor volumes to conform the dose [10].

Thus, 3D-CRT treatments are basically depends on three-dimensional anatomic information. The dose distributions in 3D-CRT conform as closely as possible to the target volume. Maximum possible dose are given to the tumor volume and the minimum possible dose to normal tissue. Clinical objectives such as maximizing tumor control probability (TCP) and minimizing normal tissue complication probability (NTCP) are also included in conformal dose distribution concept. Thus, the 3D-CRT technique includes both the physical and the biological observables [12].

IMRT is one of the most advanced radiotherapy processes in which radiation doses can be delivered highly precisely to malignant tumors of any physical shape. It is a great technical system combined with linear accelerators, sophisticated

Pradip Deb is with the Discipline of Medical Radiations, School of Medical Sciences, RMIT University, Bundoora West Campus, Victoria 3083, Australia (Phone: 61-3-99257324; fax: 61-3-99257466; e-mail: pradip.deb@rmit.edu.au).

medical imaging devices and computer guided analytical software. Due to its very high conforming capacity, very rapidly IMRT is becoming the major radiation delivery process in radiation centers worldwide [13], [14].

The main aim of IMRT is to deliver the highest possible dose of radiation to the target volume and at the same time to deliver the lowest possible dose of radiation to the surrounding normal tissues. In IMRT, a number of radiation beams are delivered to the target from a number of different directions. The beams are optimized to meet the aim of highest tumor control and normal tissue sparing. The treatment planning programs divide each radiation beam into a large number of small beams. Then the optimum setting of their radiation weights are determined. In the optimization process, the intensities of the beams are adjusted according to the dose distribution criteria for the treatment plan. This intensity adjustment are done using the inverse planning system [12]

A number of computer systems and technical methods have been devised to calculate optimum intensity profiles [11], [15]-[23]. The patient input data, i.e., three dimensional image data, image registration, segmentation etc. are required for IMRT planning. For each target the plan criteria use maximum dose, minimum dose, and dose-volume histograms. For critical structures the program requires the desired limiting dose and a dose-volume histogram.

Optimization of intensity profiles in IMRT is based on inverse planning. Although several computer programs are available and continuous updating are going on, the methods can be categorized into two major streams - analytic method and iterative method. Analytic methods use the reverse method of computed tomography (CT) reconstruction algorithm where two dimensional images are constructed from one dimensional intensity functions. The desired dose distribution is inverted by using a back projection algorithm. Thus analytic methods involve complex mathematical techniques. On the other hand in iterative methods optimizations are achieved in a different way. In iterative methods beams are iteratively adjusted to minimize the value of a cost function. The optimization process are kept going until the desired goals are met.

Radiobiology is concerned with the response of both tumors and normal tissues to irradiation. When radiation applied - both the tumor cells and normal cells are affected. But tumor cells do not have the same repair mechanism as normal cells have. By altering total dose of radiation and/or the fractionation of the scheduling, the tumor control and the normal cell sparing can be achieved [24]. Radiobiology is becoming a very important deciding factor in radiotherapy planning.

In this study a comparison between different treatment plans in radiotherapy using radiobiological models are presented. 3D-CRT and IMRT treatment plans are developed for a prostate cancer patient. Then the plans are evaluated and the radiobiological responses TCP and NTCP for the different plans are compared.

II. Methods

In this study, a radiobiological model has been used to compare 3D-CRT and IMRT treatment plans for a prostate cancer patient. Two 3D-CRT treatment plans (one with 4 fields, another with 5 fields) and an IMRT treatment plan were developed for a case of prostate cancer. Pinnacle3 Planning (Pinnacle v7.6c, Philips Medical Systems, USA) systems were used to plan and evaluate the radiobiological probabilities. The detail methods are given in the following subsections.

A. Radiobiological Model

Radiobiological models describe the dependence of tumor and normal tissue responses on the irradiated volume and dose-time-fractionation schedule. There are mathematical models for estimating TCP, NTCP, and complications free tumor control probability (P+) [11], [25]-[28].

1. Linear Quadratic Model

The linear-quadratic (LQ) model is widely used in radiotherapy in many different forms [29]. The basis of the LQ model is that a cell is inactivated only when both strands of a DNA molecule of both arms of a chromosome are damaged. This can be produced either during the passage across the cell of a single ionizing particle or by independent interactions by two separate ionizing particles.

Single-particle events can be represented by Poisson statistics. If α is the average probability per unit dose of D that a single-particle event will occur, the mean number of hits/cell is αD. So, the probability of no events is given by [30],

$$S = \exp(-\alpha D) \tag{1}$$

For the two separate ionizing particle events of the LQ model, the mean probability of one particle causing a lesion is linearly proportional to dose, as also is the mean probability that a second particle will have such an interaction. Therefore the mean probability of both events occurring is βD^2, where, β is the mean probability per unit square of the dose that such complementary events will occur. So, the probability that no such two-particle events will occur is given by:

$$S = \exp(-\beta D^2) \tag{2}$$

The overall LQ equation for cell survival is therefore:

$$S(D) = \exp(-\alpha D - \beta D^2) \tag{3}$$

S(D) is the fraction of cells surviving a dose D, α is a constant describing the initial slope of the cell survival curve, and β is a smaller constant describing the quadratic component of cell killing. The ratio α/β gives the dose at which the linear and quadratic components of cell killing are equal.

2. LQ Model for Biologically Effective Doses

Taking log of both sides of the overall LQ equation for cell survival

$$\begin{aligned} &\log S(D) = -\alpha D - \beta D^2 \\ &\Rightarrow -\log(S) = \alpha D + \beta D^2 \\ &\Rightarrow E = \alpha D + \beta D^2 \end{aligned} \quad (4)$$

where, E = -log(S), an effect. For n fractions of dose with a fraction size D,

$$E = n(\alpha D + \beta D^2) = nD(\alpha + \beta D) \quad (5)$$

If total dose = D_T, nD = D_T. Then,

$$\begin{aligned} &E = D_T(\alpha + \beta D) \\ &\Rightarrow E = D_T\alpha(1 + \frac{\beta}{\alpha}D) \\ &\Rightarrow \frac{E}{\alpha} = D_T(1 + \frac{D}{\alpha/\beta}) \end{aligned} \quad (6)$$

can be written in words as: Biologically Effective Dose (BED) = Total Dose × Relative Effectiveness (RE) [24], [31]-[33].

3. α/β Ratio

As indicated earlier in this section, the ratio α/β gives the dose at which the linear and quadratic components of cell killing are equal. If we use this concept in (3), we get,

$$\alpha D = \beta D^2 \Rightarrow \alpha/\beta = D \quad (7)$$

The parameter α/β represents the characteristics of a cell survival curve. The higher value of α/β ratio indicates the straighter the curve, meaning higher irreparable damage on the other hand smaller value of α/β indicates little irreparable damage. The great advantage of using this parameter in radiobiological models is that tumor cells tend to have higher α/β value than that of normal cells. That means tumor cells are less repairable after irradiation while normal cells can repair their damages due to radiation hit if they get enough time. Here come the fractionations. Between each fraction of radiation dose - normal tissues can be repaired. This is a very important mechanism for sparing the normal tissues while irradiating the tumor volumes.

4. Quantitative Radiobiological Model for Plan Evaluation

Advanced treatment optimization is possible using quantitative radiobiological dose response models [34]. Radiobiological models can quantify the radiobiological responses of heterogeneous tumors and organized normal tissues to non-uniform radiation dose delivery as accurately as possible. These responses are very important to optimize the treatment outcome and to find the right balance between the cure and complications. With effective radiobiological models it is possible to plan the intensity-modulated dose delivery to maximize the complication-free cure and at the same time minimize the risk of including severe normal tissue side effects.

In order to compare different treatment plans and different trials within the plan, radiobiological models are very useful. The predictive power of the models is assessed through analysis of complications of control data before they can be considered reliable for clinical treatment planning. Radiotherapy treatment plan evaluation relies on an implicit estimation of the TCP and NTCP arising from a given dose distribution. A potential application of radiobiological modeling to radiotherapy is the ranking of treatment plans via a more explicit determination of TCP and NTCP values.

5. TCP Calculations

TCP is the probability that the tumor is completely eradicated. Radiation therapy plan represents a volumetric and temporal distribution of radiation dose. The TCP value for a given tumor volume is calculated using:

$$P_i^j = e^{-\exp(e\gamma^j - \alpha^j d_i - (\beta^j d_i^2)/n)} \quad (8)$$

where $P_I{}^j$ is the probability to achieve tumor control in voxel i for tumor j, γ is the normalized slope of the dose response curve, d_i is the dose fraction at the voxel i, n is the number of fractions, α/β is the survival curve shape parameter. α/β is approximately 3 Gy for normal tissues and 10 Gy for most of the tumors. However, for a prostate tumor there is speculation that the value is much smaller as discussed in the following section. α is generated using the following equation:

$$\alpha^j = \frac{e\gamma^j - (\ln\ln 2)\frac{D_{50}^j}{nd}}{(1 + (\bar{d}/(\alpha/\beta)^j))D_{50}^j} \quad (9)$$

β is generated using:

$$\beta^j = \frac{e\gamma^j - (\ln\ln 2)\frac{D_{50}^j}{nd}}{(\bar{d} + (\alpha/\beta)^j)D_{50}^j} \quad (10)$$

where D_{50} is the dose level to achieve a 50% probability of tumor control. d is approximately 2 Gy per fraction. The composite value for all TCP responses is calculated using:

$$P_B = \prod_j P_B^j \quad (11)$$

where P_B is the overall probability for benefit of the treatment by destroying all j tumors.

6. NTCP Calculations

The NTCP value for a given organ is calculated using:

$$P_I^j = \left(1 - \prod_{i \in V^j}[1 - (P_i^j)^{s^j}]^{\Delta v_i^j}\right)^{1/s^j} \quad (12)$$

where, P_I^j is the probability of causing normal tissue complication for organ j, s^j is the relative seriality of the organ j, P_i^j is calculated using (8), V^j is the index set for the voxels covered by organ j, Δv_i^j is the relative volume calculated using:

$$\Delta v_i^j = \frac{v_i^j}{\sum_{i \in V^j} v_i^j} \quad (13)$$

The composite value for all NTCP responses is calculated using:

$$P_I = 1 - \prod_{j \in I_0} (1 - P_I^j) \quad (14)$$

where P_I is the overall probability of injury to normal tissue.

7. Complication Free Tumor Control Probability (P+)

The complication free tumor control probability (P+) i.e., composite response value [35] is generated from the combined NTCP and TCP response values. The P+ value is calculated using:

$$P_+ = P_B - P_I \quad (15)$$

where, P_B and P_I are the composite values for all TCP and NTCP given by (11) and (14) respectively.

8. Kallman S-Model

Kallman et al. [36] described the dose-volume response of tumors and normal tissues in terms of 'parallelity' and 'seriality' introducing a new parameter 'relative seriality', *s*, of the infrastructure of the organ. The radiobiological models involving parameter 's' are known as Kallman S-Model. The parameter is used in (12) for calculating NTCPs. The equations for the calculations of TCP, NTCP and P+ are all within Kallman S-Model which is used in Pinnacle Planning Systems.

B. 3D-CRT Planning

3D-CRT is a complex process. At first individual 3D digital data sets of tumors and normal adjacent organs are created. These data sets are then used to generate 3D computer images and to develop complex plans to deliver highly conformed radiation while sparing normal adjacent tissues. Because higher doses of radiation can be delivered to cancer cells while significantly reducing the amount of radiation received by surrounding healthy tissues, the technique should increase the rate of tumor control while decreasing side effects.

The treatment planning of 3D-CRT requires the availability of 3D anatomic information and a treatment planning system that allows optimization of dose distribution in accordance with the clinical objectives. In the case that considered here, the anatomic information is obtained in the form of closely spaced transverse images – CT scans. The visible tumor, critical structures and other relevant landmarks are outlined slice-by-slice.

1. Tumor Volume Determination

The most important component of the 3d-CRT process is to identify the exact position of the tumor and the exact volume of the area that to be treated [10]. The prostate and the surrounding organs at risk are outlined according to International Commission on Radiation Units and Measurements (ICRU) Reports 50 and 62 [37], [38].

The ICRU has defined several regions related to the tumor. The Gross Tumor Volume (GTV) is the gross palpable or visible/demonstrable extent and location of malignant growth [37]. Clinical experience indicates that around the GTV there are generally individual malignant cells, small cell clusters, or micro-extensions, which cannot be detected by the staging procedures. The volume surrounding the macroscopic tumor has usually a high tumor cell density close to the edge of the GTV with decreasing density towards the periphery of this volume. The GTV together with the surrounding volume of local subclinical involvement is defined as the Clinical Target Volume (CTV).

To ensure that all tissues included in the CTV receive the prescribed dose, one has to plan to irradiate a geometrically larger volume than the CTV which leads to the concept of the Planning Target Volume (PTV). A number of factors are considered while determining the PTV, such as; movements of the tissues which contain the CTV (e.g., with respiration), as well as movements of the patient, variations in size and shape of the tissues that contain the CTV (e.g., different fillings of the bladder), variations in beam geometry characteristics (e.g., beam sizes, beam directions).

According to ICRU Report 50 [37], the PTV is a geometrical concept, and it is defined to select appropriate beam sizes and beam arrangements, taking into consideration the net effect of all the possible geometrical variations, in order to ensure that the prescribed dose is actually absorbed in the CTV.

2. Organs at Risk (OAR)

Organs at risk are normal tissues whose radiation sensitivity may influence treatment planning and/or prescribed dose [37]. According to ICRU Report 62 [38], margins should be applied to organs at risk (OAR) resulting in the so-called planning organ at risk volume (PRV). So far, very few papers have discussed the use of the PRV and it appears that the concept is not much used in clinical practice [39]-[41]. Here, PTV is determined with the OAR volumes determined. The prostate is bounded superiorly by the bladder and posteriorly by the rectum. These organs are at risk during the radiation application process. Right and left femur heads may also influence the treatment planning and prescribed dose. The volumes of these organs are determined and shown in Fig. 1.

3. Beam Determination

The next step involves the use of the 3D treatment-planning software to design fields and beam arrangements. The 3D Treatment Planning System, Pinnacle v7.6c (Philips Medical Systems) has been used for the whole planning and plan evaluation process. Beam directions are chosen and the beam aperture boundaries are defined according to 3D based target and anatomic information. The beam's eye view (BEV) projection [42] is the most prominent mechanism for interactively determining beam directions and defining beam apertures [10], [12]. In 3D-CRT planning two different sets of

beam settings are designed. 4 photon beams are used in one plan and in other plan 5 photon beams are used. The main intention of using 4 beams and 5 beams in 3D-CRT is to investigate the differences due to number of beams and the beam angles. In fact, basic difference between the two plans in 3D-CRT is the number of beams and beam angles.

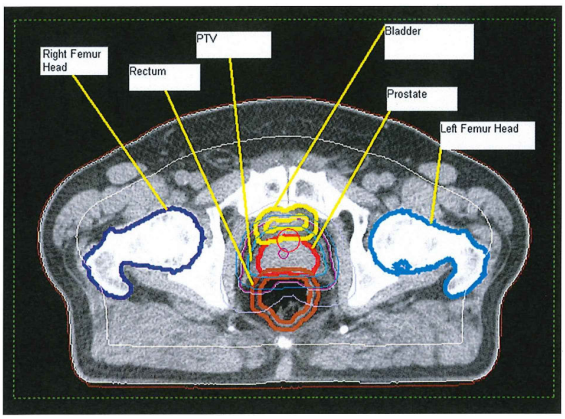

Fig. 1 The gross tumor volume (GTV: prostate), planning target volume (PTV) and the organs at risk (OAR) of patient with prostate cancer

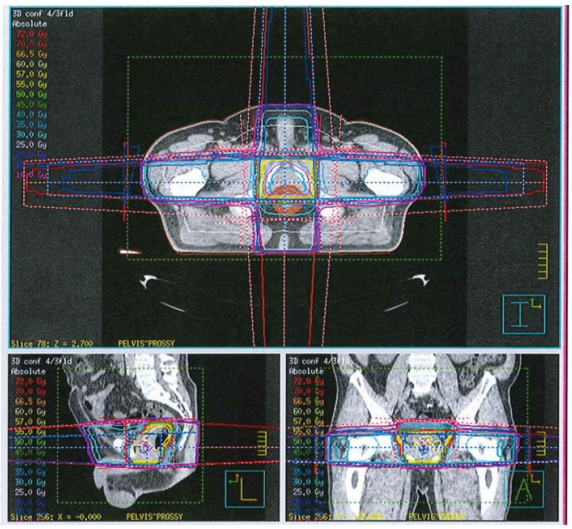

Fig. 2 Isodose curves, treatment beams, and the regions of interests of a prostate 3D-CRT 4 Fields treatment plan in three image sections, transverse (top panel), sagittal (bottom left panel), and coronal (bottom right panel) planes

4. Prescription Dose for 3D-CRT 4 Fields Plan

In the 3D-CRT 4 Fields plan a range of doses from 60 Gy to 70 Gy are used in different trials. A total of 15 trials are considered with different doses and fraction numbers and sizes. In the first 10 trials the prescription doses are planned in 30 fractions and the dose per fraction increased. In trials 11 to 15, the dose per fraction were kept constant at 2 Gy and the number of fractions increased therefore increasing the total dose. Dose distributions along with the four treatment beams on the regions of interests are shown in Fig. 2.

5. Prescription Dose for 3D-CRT 5 Fields Plan

In 3D-CRT 5 Fields plan, the same prescription doses were used as in 3D-CRT 4 fields plan for the same number of trials. Five photon beams were designed to deliver the prescription dose. The target and OAR volumes are also the same as 3D-CRT 4 fields plan shown in Fig. 1.

The treatment beams are shown along with the regions of interests in Fig. 3. The upper panel shows the transverse plane, the bottom left panel shows the sagittal plane, and the bottom right panel shows the coronal plane. Superimposing dose distributions on transverse, sagittal, and coronal planes are displayed and dose distributions along with the five treatment beams on the regions of interests are also shown in Fig. 3.

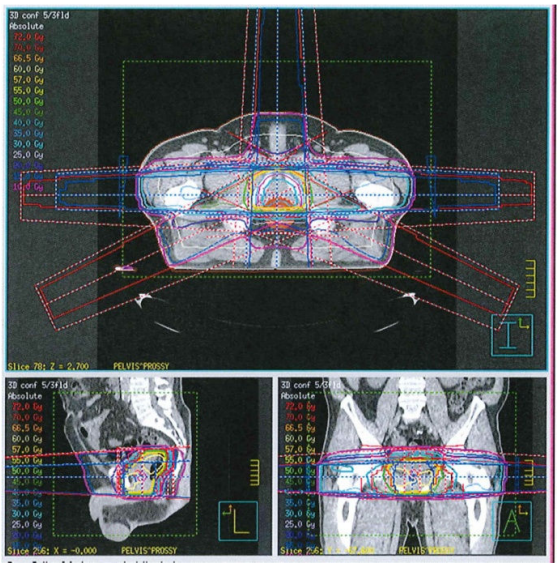

Fig. 3 As for Fig. 2, but for 3D-CRT 5fields plan

C. IMRT Planning

IMRT is an advanced three dimensional conformal treatment process. Non-uniform beam intensity patterns are used in IMRT with computer aided optimization program to achieve superior dose distribution. IMRT is capable of manipulating individual ray intensities within each beam and thus has greater control of dose distributions. IMRT is able to produce much higher conformity of dose distributions than those achievable with conventional 3D-CRT by using uniform beam intensities. The radiation dose is designed to conform to the 3D shape of the tumor by modulating or controlling the intensity of the radiation beam. Then the beam is focused to deliver a higher radiation dose to the tumor while minimizing radiation exposure to surrounding normal tissues. Treatment is carefully planned by using 3D computed tomography (CT) images of the patient. Computerized dose calculations are used to determine the dose intensity pattern that will best conform to the tumor shape. Typically, combinations of several intensity-modulated fields coming from different beam directions produce a customized radiation dose that maximizes tumor dose while also minimizes dose to the adjacent normal tissues [12], [13], [43]-[46].

In this project, the Philips Pinnacle v7.6c planning software has been used. Pinnacle is one of the four most popular IMRT planning systems in use by radiation oncology departments [47].

1. Tumor Volume Determination for IMRT

After the radiation oncologists determine the treatment targets (CTVs), a supplemental margin is added to allow the uncertainties related to the movement of the tumor volume from treatment to treatment and for potential intra-fraction organ motion. This margin establishes the PTVs [48], [49]. ICRU Report 62 [38] proposed the concept of planning organ-at-risk volume, which is a margin around the organ at risk to account for uncertainties in determining the position of the organ during actual treatments.

The target volume and the treatment planning volumes including the volumes for organ-at-risk determined in the IMRT plan that has been used here in this project are the same prostate and other organ volumes as used in 3D-CRT plans as shown in Fig. 1.

2. Beam Configuration for IMRT

Beam configuration is usually required before performing the in-field beam intensity optimization in linac based fixed-beam delivery system. Beam angle selection may have a considerable impact on the quality of the final optimized IMRT plans. But beam angle optimization might not be very important when a large number of beams are used. Here 5 photon beams are used for the IMRT plans. The beam angles in IMRT and 5fields 3D-CRT are different. The plans were created without having the beam angles fixed. It might have impacts in the comparative studies between the 3D-CRT and IMRT plans. But IMRT has high degree conformity, so beam orientation should not be a major dominating factor.

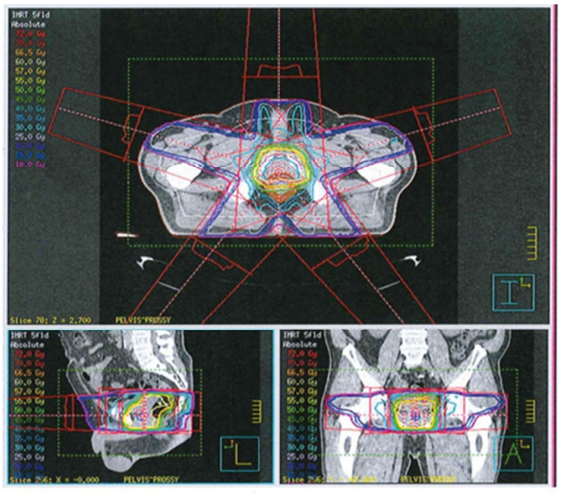

Fig. 4 As for Fig. 3, but for IMRT plans

3. Prescription Dose for IMRT

In IMRT 5 Fields plan, the same prescription doses are used for the 15 different trials as used in 3D-CRT 4 and 5 field plans. The planned fraction size and fraction numbers are also the same as 3D-CRT plans. The regions of interest, treatment beams and the isodose curves are shown in Fig. 4.

4. Biological Response Calculations

Radiotherapy planning software Philips Pinnacle v7.6c has been used to calculate the biological responses in this study. The responses are evaluated using the Kallman S-model [36], [50]. The mathematical formula used to calculate TCP, NTCP and P+ are given in (11), (14) and (15) respectively.

5. Sensitivity of the Radiobiological Evaluation to α/β Parameter

The ratio α/β is an inverse measure of a tissue's sensitivity to fractionation, that is, the size of dose given in each treatment [51]. There are many different opinions about the value of α/β for prostate tumor. According to many studies, it has been suggested that α/β values lie between as low as 1 to as high as 5 [14], [24], [52]-[64]. But as a rule of thumb, radiobiological plan evaluation software, like Pinnacle, use a typical value of $\alpha/\beta = 3$ for normal tissues and $\alpha/\beta = 10$ for tumors. The typical range in values corresponds respectively to late responding tissue for low α/β values, which has a high repair capacity, through to acute responding tissue for high α/β values which has a low repair capacity. The relative failure of small radiation doses per fraction in controlling prostate cancer might be due to hypoxia [65].

To investigate the impacts of α/β ratio, TCPs are calculated for a range of values for the ratio. Here, TCPs are calculated for different prescription doses in 3D-CRT 4 fields, 3D-CRT 5 fields, and IMRT plans using $\alpha/\beta = 1$, 1.5, 2, 2.5, 3, 4, 5, and 10.

III. Result and Discussion

The radiobiological results obtained for the different trials in three different plans are given in the following sections. For each plan, dose distribution statistics, dose volume histograms are given. Then calculated radiobiological responses, TCPs, NTCPs, and P+ for three different plans are compared.

A. TCP for Fixed Number of Dose Fractions

Tumor control probabilities calculated in three different treatment plans for different values of α/β are plotted against different prescription doses ranging from 60 Gy to 70 Gy planned in 30 fractions in Figs. 5 and 6.

Lines with diamond signs represent TCPs obtained from 3D-CRT 4 fields plan, while lines with square and triangle signs represent those obtained from 3D-CRT 5 fields and IMRT plans respectively. All of the prescription doses are planned in 30 fractions. That means the fraction size increases as the total dose increases.

TCPs obtained from IMRT plans are superior to those obtained from 3D-CRT 4 fields and 3D-CRT 5 fields for all prescription doses up to 68 Gy. Above 65 Gy, all three plans give almost same TCP. From dose range 63 to 65 Gy, the two 3D-CRT plans give almost same TCPs. At the prescription dose ranged 60 Gy to 63 Gy, IMRT plans give the highest TCP, while 3D-CRT 4 fields plans show the lowest TCPs

among the three plans considered, although the difference is within 2%. It is evident for all three plans that the TCP increases while the prescription dose is increased. At a prescription dose of 60 Gy, the TCP is about 86.5% for 3D-CRT 4 fields plan, while those from 3D-CRT 5 fields and IMRT plans are 87% and 88.5% respectively. But for a prescription dose of 70 Gy, TCPs from 3D-CRT 4 fields, 3D-CRT 5 fields and IMRT plans are increased to more than 99%. Since the differences in TCPs obtained in three plans are very small, we have to look at the corresponding NTCP for these plans to find out which plan is more acceptable for normal tissue sparing.

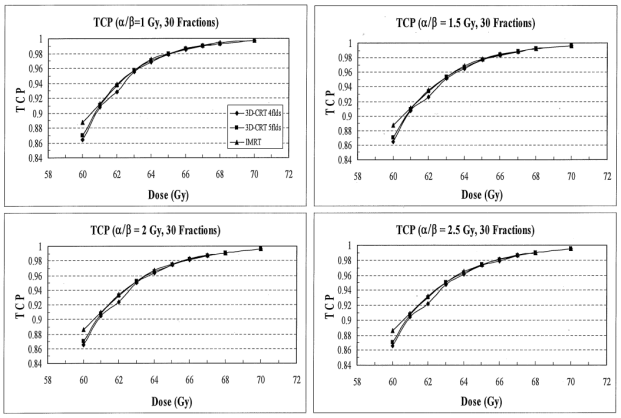

Fig. 5 TCP as a function of prescription dose planned in 30 fractions in 3D-CRT 4 field (diamond), 3D-CRT 5 field (square), and IMRT (triangle) plans for α/β = 1, 1.5, 2 and 2.5 Gy. Lines between the data points are as visual guide only

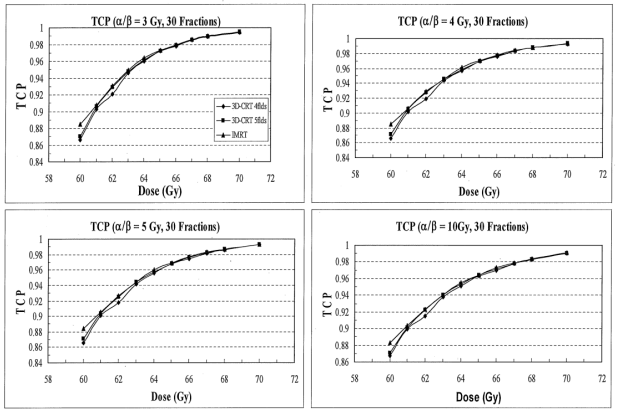

Fig. 6 As for Fig. 5, but for α/β = 3, 4, 5 and 10 Gy.

B. TCPS for Fixed Size of Dose Fractions

Tumor control probabilities calculated in three different treatment plans for different values of α/β are plotted against different prescription doses ranging from 60 Gy to 70 Gy planned in 2 Gy per fraction in Figs. 7 and 8. The total dose is increased by increasing the number of 2 Gy/fraction.

Lines with diamond signs represent TCPs obtained from 3D-CRT 4 fields plan, while lines with square and triangle signs represent those obtained from 3D-CRT 5 fields and IMRT plans respectively. Fig. 7 shows the results obtained for α/β = 1, 1.5, 2, and 2.5 Gy. Fig. 8 shows those obtained for α/β = 3, 4, 5, and 10 Gy.

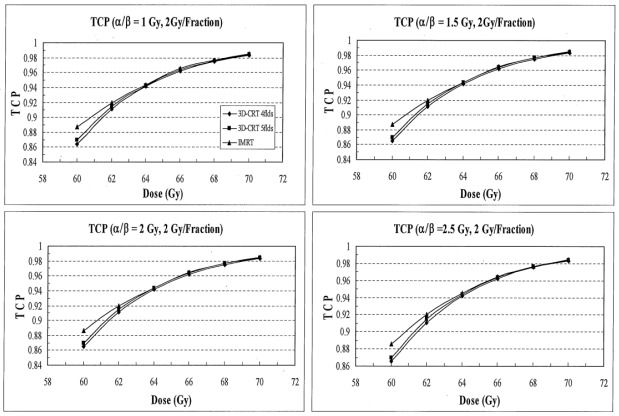

Fig. 7 TCP as a function of prescription dose planned in 2 Gy per fraction in 3D-CRT 4field (diamond), 3D-CRT 5field (square), and IMRT (triangle) plans for α/β = 1, 1.5, 2, and 2.5 Gy. The lines between the data points are for visual guidance only

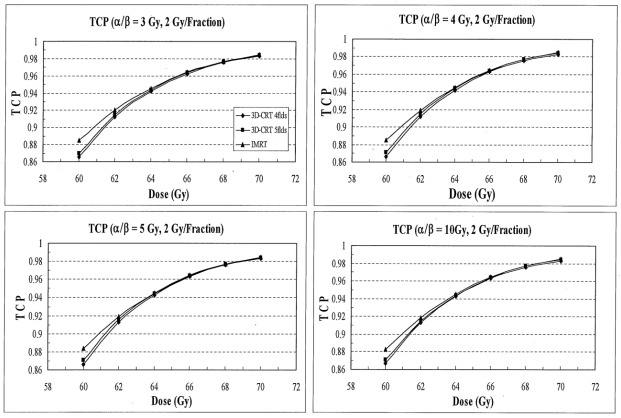

Fig. 8 As for Fig. 7, but for α/β = 3, 4, 5 and 10 Gy

TCPs obtained from IMRT plans are superior to those obtained from 3D-CRT 4 fields and 3D-CRT 5 fields for all prescription doses up to 70 Gy. Above 66 Gy, all three plans give almost same tumor control probabilities. From dose range 66 to 68 Gy, the two 3D-CRT plans give almost same TCPs. At the prescription dose ranged 60 Gy to 64 Gy, IMRT plans give the highest TCP, while 3D-CRT 4fields plans show the lowest TCPs among the three plans considered, although the difference is within less than 2%. It is evident for all three plans that the TCP increases while the prescription dose is increased. At a prescription dose of 60 Gy, the TCP is about 86.5% for 3D-CRT 4 fields plan, while those from 3D-CRT 5 fields and IMRT plans are 87% and 89% respectively. But for a prescription dose of 70 Gy, TCPs from 3D-CRT 4 fields, 3D-CRT 5 fields and IMRT plans are increased to more than 98%. It is noticeable that at a prescription dose of 70 Gy, TCPs are more than 99 % for all the three plans when fraction size is 2.33 Gy (30 fractions), but TCPs are slightly smaller

(98%) when fraction size is 2 Gy. The impacts of fraction size on TCPs are discussed in the following section.

C. Impacts of Fraction Size on TCP

As we have seen TCPs obtained from two different categories of fractionation are slightly different. In Fig. 9, TCPs are presented as a function of prescription dose planned (I) in 30 fractions and (II) in 2 Gy per fraction for $\alpha/\beta = 1$, 1.5, 2, and 2.5 in three treatment plans, while those for $\alpha/\beta = 3$, 4, 5, and 10, are presented in Fig. 10. Solid lines show TCPs obtained when prescription doses are planned in 30 fractions. Dotted lines show TCPs when the prescription doses are planned in 2 Gy per fraction. Different marks on the lines indicate different treatment plans. Diamonds represent 3D-CRT 4 fields plan, while squares and triangles represent 3D-CRT 5 fields and IMRT plans respectively.

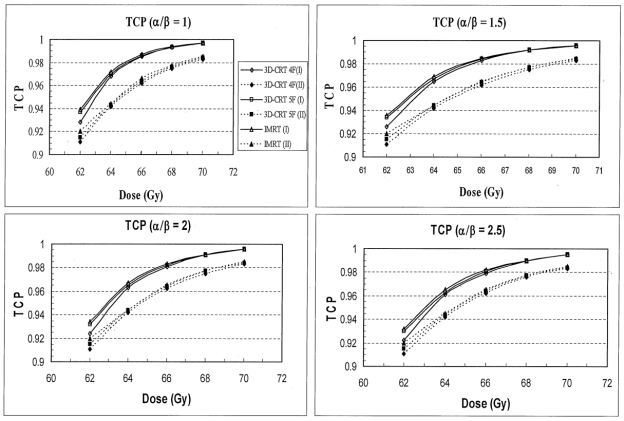

Fig. 9 TCP as a function of prescription dose planned (I) in 30 fractions (solid line) and (II) in 2 Gy per fraction (dotted line) in 3D-CRT 4field (diamond), 3D-CRT 5field (square), and IMRT (triangle) plans for $\alpha/\beta = 1$, 1.5, 2, and 2.5 Gy. Lines between the data points are used as visual guide only

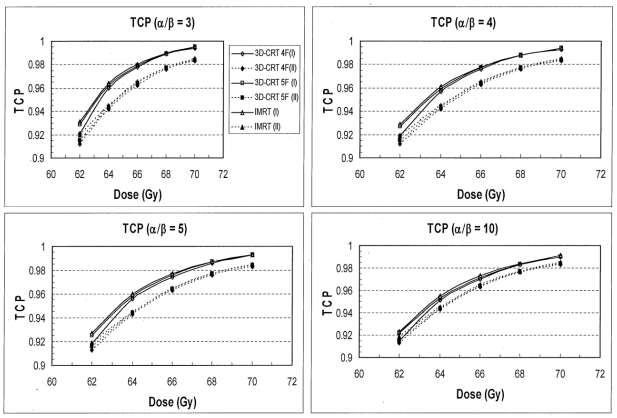

Fig. 10 As for Fig. 9, but for $\alpha/\beta = 3$, 4, 5, and 10 Gy

In all cases, TCPs obtained for the fixed fraction size are smaller by about 1% than those for increased fraction sizes. Despite the difference due to fraction sizes, in all trials and plans, IMRT gives the highest TCPs. The difference due to fraction size increased at prescription dose ranged between 62 and 66 Gy. This difference gradually decreases when the prescription dose increases as TCPs tend to 100%. TCPs are not very sensitive to α/β values when fraction size is fixed, but quite noticeable when fraction size changes. If α/β is in fact low, then changing the fraction size has an effect on the calculated TCP. If α/β is high then total dose is the important parameter, not dose/fraction.

D. Normal Tissue Complication Probability (NTCP)

The performance of the treatment plans are evaluated by looking at their corresponding NTCPs. A lower NTCP means a higher probability of normal tissue sparing. As we have seen in the previous sections that at a certain prescription dose level all the three plans result in nearly equal TCPs. So NTCPs play a deciding role for the complications free tumor control probability.

Calculated NTCPs for different treatment plans are compared with each other in this section. NTCPs are plotted as a function of prescription dose. To investigate the effects of fraction size, prescription doses are planned to be escalated by either increasing the number of fractions for a fixed dose/fraction, or increasing dose/fraction for a fixed number of fractions. NTCPs are compared for both the categories.

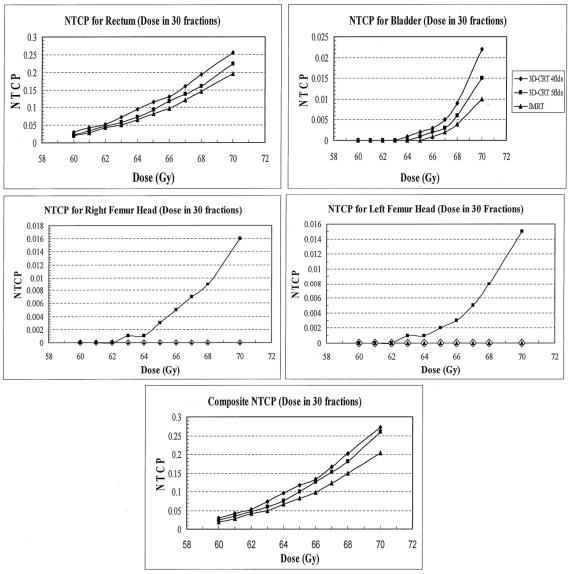

Fig. 11 NTCPs for rectum, bladder, right and left femur heads, and composite NTCP as a function of prescription dose in 3D-CRT 4field (diamonds), 3D-CRT 5field (squares) and IMRT (triangle) plans when the doses are planned in 30 fractions. Lines between the data points are to guide the eye only

1. NTCP for Fixed Number of Dose Fractions

In Fig. 11, NTCP for rectum, bladder, right and left femur heads, and composite NTCP are plotted as a function of prescription dose planned in 30 fractions in 3D-CRT 4 fields (diamonds), 3D-CRT 5 fields (squares) and IMRT (triangle) plans. Symbols on the solid lines indicate different treatment

plans. Diamonds, squares and triangles indicate 3D-CRT 4 fields, 3D-CRT 5 fields, and IMRT plans respectively.

The rectum absorbs large amounts of radiation which cause tissue complications. Modern treatment plans are designed to address this issue. NTCPs for rectum obtained from the three treatment plans are presented in the top left panel of Fig. 11. 3D-CRT 4fields plan results in the highest NTCP, while IMRT plans give the lowest NTCP for all of the prescription doses. Normal tissue complications increased with prescription dose. At 60 Gy, NTCP for all the three plans are within the range of 2 to 3%, but increased to 20 to 26% for the prescription dose of 70 Gy. At 70 Gy, 3D-CRT 4 fields plan introduce tissue complications by 26%, while IMRTs NTCP is about 20%. IMRT performs better than the other two 3D-CRT plans on the basis of limiting the tissue complications in rectum.

NTCPs for bladder are given in the top right panel of Fig. 11. From the figure, we see NTCP for bladder is zero for the total dose of up to a level of 63 Gy. Complications start as the dose increased up to 63 Gy. Again, IMRT gives the lowest NTCPs while 3D-CRT 4 fields plan gives the highest NTCP. At 70 Gy, NTCP for 3D-CRT 4 fields plan is about 2.2%, for 3D-CRT 5 fields that is 1.5% while it is only 1% for IMRT.

NTCPs for right and left femur heads are given in the middle left and middle right panels of Fig. 11 respectively. 3D-CRT 4 fields and IMRT plans do not cause any complications to the femur heads at any level of prescription dose up to 70 Gy. But 3D-CRT 5 fields cause normal tissue complications to the femur heads. At 70 Gy, NTCP for 3D-CRT 5 fields plan is about 1.5%. Beam alignment in 3D-CRT 5 fields plan might be a reason for the exposure of femur heads.

The composite NTCP for the four organs at risk considered are plotted in the bottom panel of Fig. 11. The major contribution comes from the rectum as its seriality is 1.5, very high compared to 0.18 for bladder. IMRT causes lowest NTCPs for the prescription dose ranged 60 to 70 Gy planned in 30 fractions, while 3D-CRT 4 fields plans give the highest. For prescribed dose 70 Gy, NTCP for 3D-CRT 4 fields is about 27%, while it is 20% for IMRT.

2. NTCPS for Fixed Size of Dose Fractions

In Fig. 12, NTCP for rectum, bladder, right and left femur heads, and composite NTCP are plotted as a function of prescription dose planned in 2 Gy per fraction in 3D-CRT 4 fields (diamonds), 3D-CRT 5fields (squares) and IMRT (triangle) plans. Symbols on the solid lines indicate different treatment plans. Diamonds, squares and triangles indicate 3D-CRT 4 fields, 3D-CRT 5 fields, and IMRT plans respectively.

NTCPs for rectum are plotted against the prescription dose planned in 2 Gy/fraction are plotted in the top left panel of Fig.12. NTCPs for IMRT are the lowest and those for 3D-CRT 4 fields are the highest. NTCPs increase with prescription dose. The differences among NTCPs for different plans at lower prescription dose are small compared to those at higher prescription doses. At 60 Gy, the range of NTCPs is 2 to 3%, while at 70 Gy, the range is 11 to 16%. At 70 Gy, NTCPs for 3D-CRT 4 fields, 3D-CRT 5 fields and IMRT plans are about 16%, 13% and 11% respectively.

NTCPs for bladder are plotted in the top left panel of Fig. 12. Again, IMRT plans give the minimum NTCPs, and 3D-CRT 4 fields plan causes the highest probability of tissue complications. Up to 64 Gy, NTCPs for all the three plans are zero, then complications start for 3D-CRT plans. The probability range is very small, 0.1% to 0.5%. At 70 Gy, NTCP for IMRT = 0.2% while those are 0.3% and 0.5% for 3D-CRT 5 fields and 3D-CRT 4 fields plans respectively.

NTCPs for femur heads are plotted in the middle panels of Fig. 12. It shows that only 3D-CRT 5 fields plans cause the complications in femur heads, which is about 0.5 % for right femur head and 0.6 % for left femur head at a prescription dose of 70 Gy.

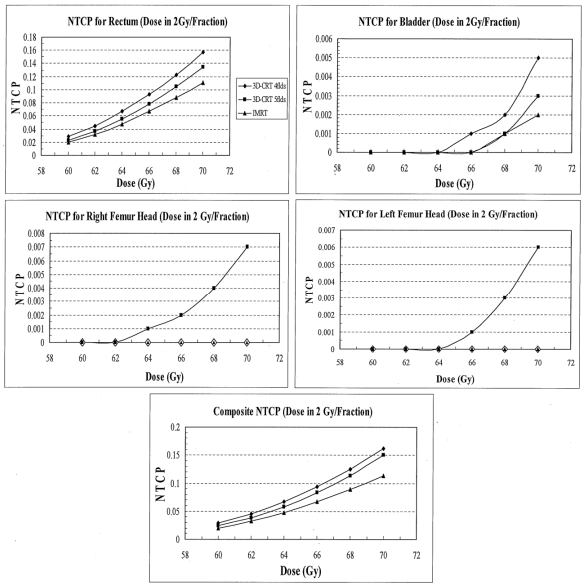

Fig. 12 As for Fig. 11, but for when the doses are planned in 2 Gy/fraction

The composite NTCPs for the organs at risk are given in the bottom panel of Fig. 12. It shows that NTCPs for IMRT are the minimum and those for 3D-CRT 4 fields are the maximum. At 70 Gy, NTCP for IMRT is about 11%, while it is 16% for 3D-CRT 4 fields. It is noticeable that NTCPs at 70 Gy planned in 2 Gy/fraction, is smaller than those when 70 Gy planned in 30 fractions.

3. Effects of Fraction Size on NTCP

NTCP calculated for three different treatment plans at different prescription doses planned in two categories: fixed number of fractions and fixed size of fractions. These two kinds of NTCPs are compared in Fig. 13 for investigating the effects of fraction sizes on NTCP. The solid lines represent NTCPs calculated for the prescription dose planned in 30 fractions, and dotted lines represent NTCPs calculated for the prescription dose planned in 2 Gy per fraction. The diamond, square, and triangle symbols on the lines indicate the

treatment plans 3D-CRT 4fields, 3D-CRT 5 fields, and IMRT respectively.

NTCPs for rectum are plotted in the top left panel of Fig. 13. It is clearly shown that NTCPs are higher when the dose are planned in 30 fractions than those when the dose are planned in 2 Gy/fraction. In fixed number of fractions, the fraction size increases with dose. In that case, when prescription dose is 60 Gy, fraction size is 2 Gy. But when prescription dose is 70 Gy, fraction size becomes 2.33 Gy. A high fraction of dose might be good for tumor control, but it causes the normal tissue complications as at that fraction of dose the cell repairing mechanism might be affected. So, if the high dose is recommended, high fraction size is not. IMRT plans show the minimum NTCPs in both fraction categories. In 2 Gy/fraction categories, NTCP for IMRT is 10%, while it is 20% for the 30 fractions category at a prescription dose of 70 Gy.

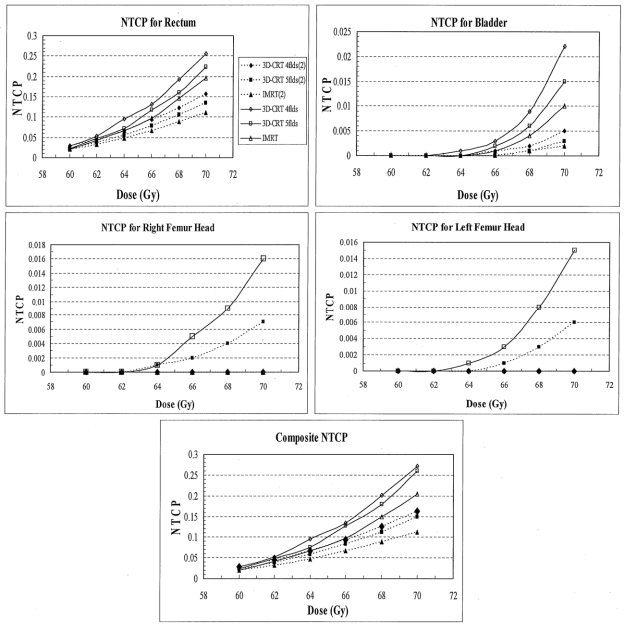

Fig. 13 NTCPs for rectum, bladder, femur heads, and composite NTCPs as a function of prescription dose planned in 30 fractions (solid line) and in 2 Gy per fraction (dotted line) in 3D-CRT 4fields (diamond), 3D-CRT 5fields (square), and IMRT (triangle) plans. Lines between the data points are for visual guidance only

NTCPs for bladder calculated in both fraction categories are plotted in the top right panel of Fig. 13. Again, for all three treatment plans, 2 Gy/fraction categories of fractionations produce lower NTCPs than NTCPs when dose are planned in 30 fractions. IMRT plans give the lowest NTCPs while 3D-CRT 4 fields plans give the highest. For IMRT, NTCP is about 0.1% when prescription dose 70 Gy planned in 2 Gy/fraction, but this value is 10 times higher (1%) when the prescription dose is planned in 30 fractions, i.e., in 2.33 Gy/fraction.

NTCPs for right and left femur heads are plotted in middle left and middle right panels of Fig. 13. Only 3D-CRT 5 fields plans causes the complications in femur tissues for the prescription dose range 62 to 70 Gy. Again, the complications become more than double when the fraction size is increased. At 70 Gy, NTCP for 3D-CRT 5 fields is 0.7% when the dose is planned in 2 Gy/fraction, but 1.6% when dose is planned in 2.33 Gy/fraction.

The bottom panel of Fig. 13 shows the composite NTCPs for the three treatment plans and for the dose planned in two categories. Since composite NTCPs are the sum of NTCPs for the individual organs at risk. Higher fraction size causes larger normal tissue complications. IMRT plans cause the minimum tissue complication probabilities.

E. Complication Free Tumor Control Probability (P+)

P+ are plotted in Figs. 14 and 15 as a function of prescription dose planned in 30 fractions for different values of α/β. The solid lines with symbols of diamonds, squares, and triangles represent P+ obtained for the treatment plans 3D-CRT 4 fields, 3D-CRT 5 fields, and IMRT respectively. From all panels of the Figs. 14 and 15, it is evident that IMRT plans show the highest P+, which means IMRT is more efficient than the other two 3D-CRT plans.

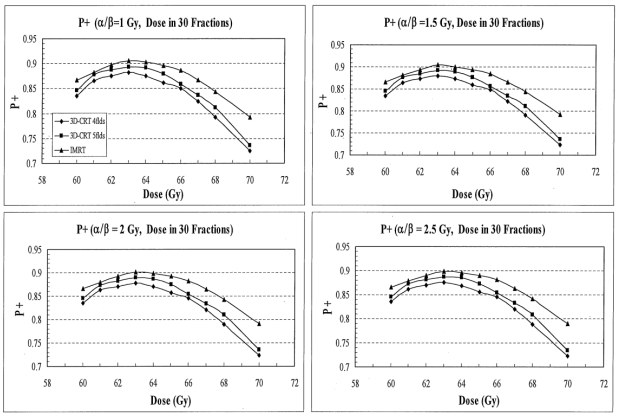

Fig. 14 P+ as a function of prescription dose planned in 30 fractions in different treatment plans for α/β = 1, 1.5, 2, and 2.5 Gy. Lines interpolate between data points as a visual guide only

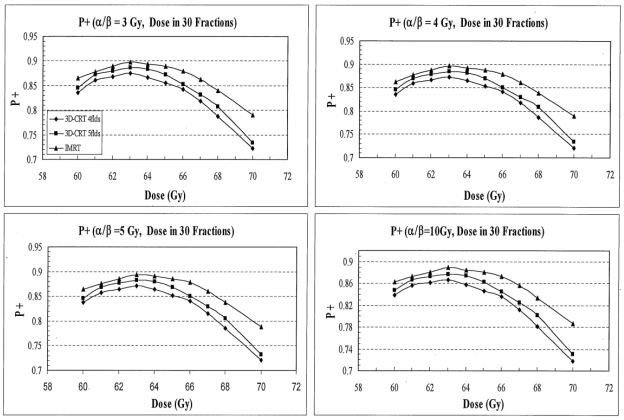

Fig. 15 As for Fig. 14, but for α/β = 3, 4, 5, and 10 Gy

P+ initially increased in all three plans with the increase of prescription dose up to 63 Gy, then decreased with the increase of prescription dose. For all the α/β values, P+ changes with the prescription dose at almost same rate for all the three plans. That means the α/β values do not much affect P+. The highest P+ is obtained for IMRT at a prescription dose of 63 Gy in the category of dose delivery in 30 fractions. For higher energies, as the fraction size increased, the composite NTCPs also increased. As a result P+ decreased. The P+ for IMRT treatment plan is 3% higher than 3D-CRT plans at low prescription dose and 6% higher than those at high doses. Undoubtedly the IMRT plan is giving the highest probability of complications free tumor control probability in this case.

2. Dose Planned in 2 GY per Fraction

Figs. 16 and 17 show P+ for 3D-CRT 4 fields, 3D-CRT 5 fields and IMRT treatment plans for the prescription dose ranged 60 Gy and 70 Gy planned in 2 Gy per fraction plotted against the prescription dose.

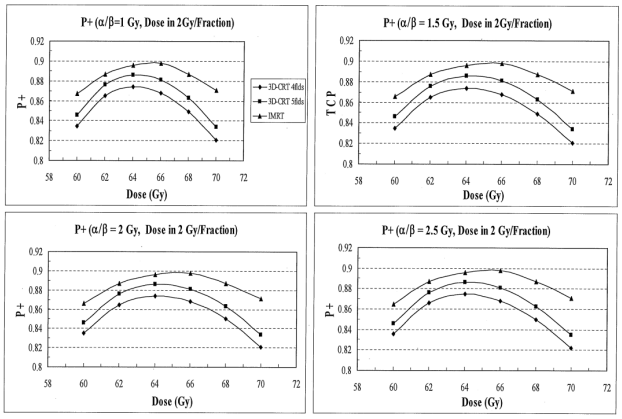

Fig. 16 P+ as a function of prescription dose planned in 2 Gy per fraction in different treatment plans for α/β = 1, 1.5, 2, and 2.5 Gy. Smooth lines between the data points are to guide the eye only

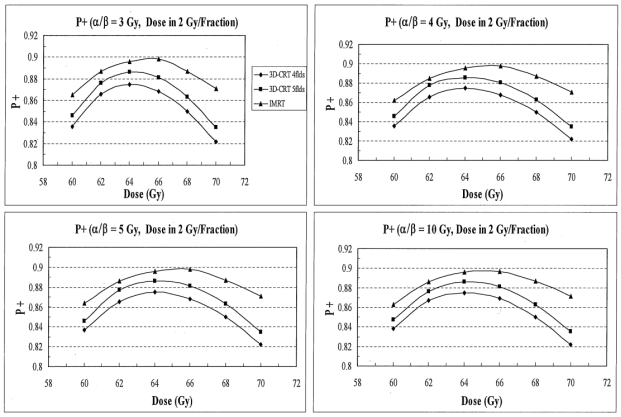

Fig. 17 As for Fig. 16, but for α/β = 3, 4, 5, and 10 Gy

Different panel of the figures represent the P+ for different values of α/β as indicated in the title of each panel. It is clearly evident that IMRT plans result with the highest P+ for all prescription doses, while 3D-CRT 4 fields plan give the lowest P+, although the difference is within 3 to 5%. The optimum values for P+ obtained for different values of α/β are at the prescription dose of 66 Gy. For higher doses, TCP increased, but NTCPs also increased resulting with overall low P+ at high prescription doses.

3. Effects of Fraction Size on P+

Fraction sizes have noticeable effects on P+. Since high fraction size increases NTCP, it lowers the P+. The results for two different types of fraction sizes used for the same prescription doses are shown in Figs. 18 and 19. The P+ for different plans is plotted against the prescription dose. Solid lines represent the P+ obtained when the dose are planned in 30 fractions, while the dotted lines show those when dose are planned in 2 Gy per fraction. At lower energies, the fraction size difference is very small, so the differences of P+ also small at that dose range. But for high dose, fraction size difference is large, 0.33 Gy for the case of 70 Gy, which cause a large NTCP. As a result P+ becomes small. Again IMRT shows the highest P+ for all cases.

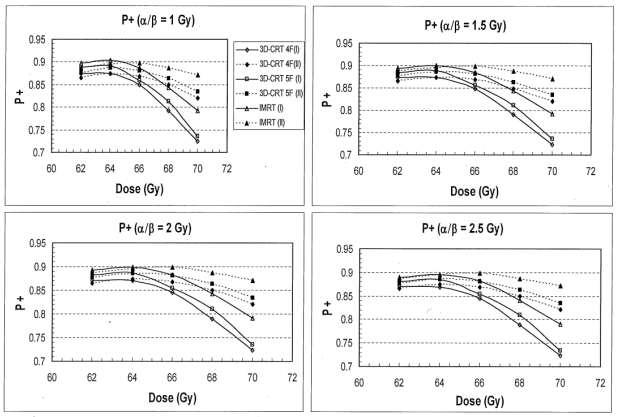

Fig. 18 P+ as a function of prescription dose planned in (I) 30 fractions and (II) 2 Gy/fraction in different treatment plans for α/β = 1, 1.5, 2, and 2.5 Gy. Trend lines between the data points are drawn to guide the eye

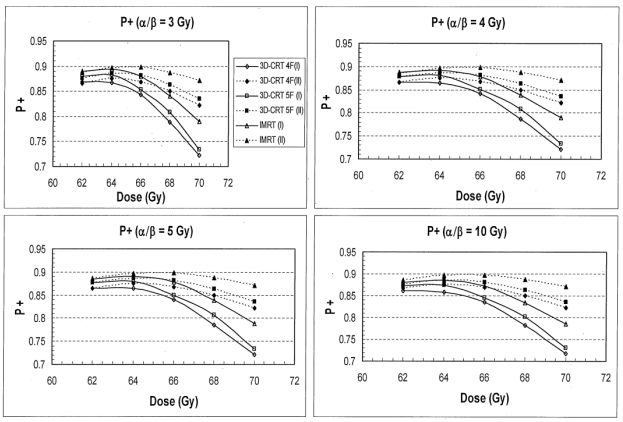

Fig. 19 As for Fig. 18, but for α/β = 3, 4, 5, and 10 Gy

IV. Conclusion

This study shows that the use of appropriate radiobiological models for treatment plan evaluation can predict the clinical outcome of radiation treatments allowing an improvement of the planned therapy. It has been found in this study, that although the IMRT and 3D-CRT plans give almost the same TCPs, IMRT plans give the minimum NTCP. So considering overall radiobiological responses, it might be claimed that IMRT is more acceptable than the other 2 plans. But there are some limitations in this study. The beam configurations of the two plans which were prepared for 3D-CRT plans are different, so differences among the outcomes of those plans might be due to beam orientations. The beam configurations for 5fields IMRT and 5fields 3D-CRT are also different. So the superior outcome of the IMRT might not be clearly justified. It will be worthy to have a further investigation with the same beam orientations in different plans. When the dose is increased, both the TCP and NTCP increased gradually as expected. P+ are higher for the IMRT plans than for the 3D-CRT plans. It supports the hypothesis that accurately planned IMRT for prostate carcinoma reduces the complication rate among the organs at risks while increasing TCP compared to standardized 3D-CRT. TCPs are comparatively more sensitive to the α/β values for the plans where the fraction numbers are kept constant than for the plans where fraction sizes are unchanged.

References

[1] Fowler, J.F., Nuclear particles in cancer treatment. Medical physics handbooks. 1981, Bristol, UK: Adam Hilger Ltd.
[2] Hirst, D.G., The importance of radiobiology to cancer therapy: current practice and future perspectives. Clinical Oncology, 2007. 19: p. 367-369.
[3] Pavone-Macaluso, M., Patient selection criteria for surgery, in Radiotherapy of prostate cancer, C. Greco and M. J. Zelefsky, Editors. 2000, Harwood Academic Publishers: Amsterdam, The Netherlands. p. 69-74.
[4] Small, W., Jr. and G. Woloschak, Introduction, in Radiation Toxicity A Practical Guide, W. Small, Jr. and G. Woloschak, Editors. 2006, Springer: Chicago, IL, USA.
[5] Hanks, G.E., et al., Conformal technique dose escalation for prostate cancer: Chemical evidence of improved cancer control with higher doses in patients with pretreatment prostate-specific antigen >10 ng/ml. International Journal of Radiation Oncology Biology Physics, 1996. 35: p. 861-868.
[6] Leibel, S.A., et al., Three-dimensional conformal radiation therapy in locally advanced carcinoma of the prostate: Preliminary results of a phase I dose-escalation study. International Journal of Radiation Oncology Biology Physics, 1994. 28: p. 55-65.
[7] Perez, C.A., et al., Three-dimensional conformal therapy (3-D CRT) and potential for intensity-modulated radiation therapy in localized carcinoma of prostate. In The Theory and Practice of Intensity Modulated Radiation Therapy. E.S. Sternick, Editor. 1997 Advanced Medical Publishing. Madison, WI, USA. p. 199-217.
[8] Perez, C.A. and J. Michalski, Outcome of external-beam radiation therapy for localized carcinoma of the prostate (stages T1B, T2, and T3). in Radiotherapy of prostate cancer, C. Greco and M.J. Zelefsky, Editors. 2000, Harwood academic publishers: Amsterdam, The Netherlands. p. 155-184.
[9] del Regato, J.A., A.H. Trailins, and D.D. Pittman, Twenty years follow-up of patients with inoperable cancer of the prostate (stage C) treated by radiotherapy: Report of a national cooperative study. International Journal of Radiation Oncology Biology Physics, 1993. 26: p. 197-201.
[10] Prado, K.L., G. Starkschall, and R. Mohan, Three-dimensional conformal radiation therapy. , in Treatment Planning in Radiation Oncology. F.M. Khan, Editor. 2007, Lippincott Williams & Wilkins: Philadelphia, PA, USA. p. 116-141.
[11] Webb, S., The Physics of Conformal Radiotherapy. 1997, Bristol, UK.: Institute of Physics Publishing.
[12] Khan, F.M., The Physics of Radiation Therapy. 3rd ed. 2003, Philadelphia, USA.: Lippincott, Williams and Wilkins.
[13] Dong, L. and R. Mohan, Intensity-modulated radiation therapy physics and quality assurance. in Practical essentials of intensity modulated radiation therapy., K.S.C. Chao, Editor. 2005, Lippincott Williams & Wilkins: Philadelphia, PA, USA. p. 1-19.
[14] Williams, M., A review of intensity modulated radiation therapy: incorporating a report on the seventh education workshop of the ACPSEM - ACT/NSW branch. Australasian Physical & Engineering Sciences in Medicine, 2002. 25(3): p. 91-101.
[15] Bortfeld, T.R., J. Burkelbach, and R. Boesecke, Methods of image reconstruction from projections applied to conformal therapy. . Physics in Medicine and Biology, 1990. 35: p. 1423-1434.
[16] 16. Brahme, A., Optimization of stationary and moving beam radiation therapy techniques. Radiotherapy Oncology, 1988. 12: p. 129-140.
[17] Convery, D.J. and M.E. Rosenbloom, The generation of intensity modulated fields for conformal radiotherapy by dynamic collimation. Physics in Medicine and Biology, 1992. 37: p. 1359-1374.
[18] Holmes, T. and T.R. Mackie, A filtered back projection dose calculation method for inverse treatment planning. Medical Physics, 1994. 21: p. 303-313.
[19] Kallman, P., B. Lind, and A. Ekloff, Shaping of arbitrary dose distribution by dynamic Multileaf collimation. Physics in Medicine and Biology, 1988. 33: p. 1291-1300.
[20] Mageras, G.S. and R. Mohan, Application of fast simulated annealing to optimization of conformal radiation treatment. Medical Physics, 1993. 20: p. 639-647.
[21] Mohan, R., G.S. Mageras, and B. Baldwin, Clinically relevant optimization of 3D conformal treatments. Medical Physics, 1992. 20: p. 933-944.
[22] Rosen, H., R.G. Lane, and S.M. Morrill, Treatment planning optimization using linear programming. Medical Physics, 1991. 18: p. 141-152.
[23] Webb, S., Optimization of conformal dose distributions by simulated annealing. Physics in Medicine and Biology, 1989. 34: p. 1349-1370.
[24] Fowler, J.F., Radiobiological principles guiding the management of prostate cancer., in Radiotherapy of Prostate Cancer., C. Greco and M.J. Zelefsky, Editors. 2000, Harwood Academic Publishers: The Netherlands. p. 131-145.
[25] Kutcher, G.J., Quantitative plan evaluation: TCP/NTCP models. , in 3-D Conformal Radiotherapy A New Era in the Irradiation of Cancer, J.L. Meyer and J.A. Purdy, Editors. 1996, Karger: Basel, Switzerland. p. 67-80.
[26] Kutcher, G.J., Quantitative plan evaluation, in Advances in Radiation Oncology Physics Dosimetry, Treatment Planning, and Brachytherapy., J.A. Purdy, Editor. 1990, American Association of Physicists in Medicine: Kansas, USA. p. 998-1021.
[27] Haken, R.K.T. and M.L. Kessler, Quantitative tools for plan evaluation, in General Practice of Radiation Oncology Physics in the 21st Century., A.S. Shiu and D.E. Mellenberg, Editors. 2000, Medical Physics Publishing: Illinois, USA. p. 17-36.
[28] Niemierko, A., Current status of TCP and NTCP calculations, in 3-D Conformal and Intensity Modulated Radiation Therapy: Physics & Clinical Applications. , J.A. Purdy, et al., Editors. 2001, Advanced Medical Publishing: Madison, WI, USA. p. 95-111.
[29] Wigg, D.R., Applied Radiobiology and Bioeffect Planning. 1st ed. 2001, Madison, Wisconsin, USA: Medical Physics Publishing.
[30] Tubiana, M., J. Dutreix, and A. Wambersie, Introduction to Radiobiology. 1990, Bristol: Taylor & Francis. 97-104.
[31] Barendsen, G.W., Dose fractionation, dose rate and iso-effect relationships for normal tissue responses. International Journal of Radiation Oncology Biology Physics, 1982. 8: p. 1981-1997.
[32] Dale, R.G., The application of the linear-quadratic dose-effect equation to fractionated and protracted radiotherapy. British Journal of Radiology, 1985. 58: p. 515-528.
[33] Fowler, J.F., The linear quadratic formula and progress in fractionated radiotherapy: a review. British Journal of Radiology, 1989. 62: p. 679-694.
[34] Brahme, A., J. Nilsson, and D. Belkic, Biologically optimized radiation therapy. Acta Oncologica, 2001. 40(6): p. 725-734.

[35] Agren, A.K., A. Brahme, and I. Turesson, Optimization of uncomplicated control for head and neck tumors. International Journal of Radiation Oncology Biology Physics, 1990. 19(4): p. 1077-85.
[36] Kallman, P., A. Agren, and A. Brahme, Tumor and normal tissue responses to fractionated non uniform dose delivery. International Journal of Radiation Biology 1992. 62(2): p. 249-262.
[37] International Commission on Radiation Units and Measurements (ICRU) Report 50, Prescribing, Recording, and Reporting Photon Beam Therapy 1993: Bethesda, MD, USA.
[38] International Commission on Radiation Units and Measurements (ICRU) Report 62, Prescribing, Recording, and Reporting Photon Beam Therapy (Supplement to ICRU Report 50). 1999: Bethesda, MD, USA.
[39] McKenzie, A., M. van Herk, and B. Mijnheer, Margins for geometric uncertainty around organs at risk in radiotherapy. Radiotherapy Oncology, 2002. 62: p. 299-307.
[40] Muren, L.P., R. Ekerold, and Y. Kvinnsland, On the use of margins for geometrical uncertainties around the rectum in radiotherapy planning. Radiotherapy Oncology, 2004. 70: p. 11-19.
[41] Stroom, J.C. and B.J.M. Heijmen, Limitations of the planning organ at risk volume (PRV) concept. International Journal of Radiation Oncology Biology Physics, 2006. 66(1): p. 279-286.
[42] Goitien, M., M. Abrahams, and D.R. Rowell, Multidimensional treatment planning: II. Beam's eye view, back projection, and projection through CT sections. International Journal of Radiation Oncology Biology Physics, 1983. 9: p. 789-797.
[43] Bortfeld, T., IMRT: a review and preview. Physics in Medicine and Biology, 2006. 51: p. R363-R379.
[44] Boyer, A.L., Intensity modulated radiation therapy, in Treatment Planning In Radiation Oncology, F.M. Khan, Editor. 2007, Lippincott Williams & Wilkins: Philadelphia, PA, USA. p. 142-165.
[45] Intensity Modulated Radiation Therapy Collaborative Working Group, Intensity-modulated radiotherapy: current status and issues of interest. International Journal of Radiation Oncology Biology Physics, 2001. 51(4): p. 880-914.
[46] Purdy, J.A., The development of intensity modulated radiation therapy, in The Theory & Practice of Intensity Modulated Radiation Therapy, E.S. Sternick, and Editor. 1997, Advanced Medical Publishing: Madison, WI, USA. p. 1-15.
[47] Peterson, L., Intensity modulated radiation therapy update. Trends in Medicine, 2003. March: p. 1-3.
[48] Purdy, J.A., Volume and dose specification for three-dimensional conformal radiotherapy. , in 3D Radiation Treatment Planning and Conformal Therapy, J.A. Purdy and B. Emami, Editors. 1995, Medical Physics Publishing: Madison, Wisconsin, USA. p. 11-14.
[49] Purdy, J.A., Dose volume specification: new challenges with intensity-modulated radiation therapy Seminars in Radiation Oncology, 2002. 12: p. 199-209.
[50] Lof, J., Development of a general framework for optimization of radiation therapy. 2000, Stockholm University: Stockholm.
[51] McAneney, H. and S.F.C. O'Rourke, Investigation of various growth mechanisms of solid tumor growth within the linear-quadratic model for radiotherapy. Physics in Medicine and Biology, 2007. 52: p. 1039-1054.
[52] Fowler, J.F., The radiobiology of prostate cancer including new aspects of fractionated radiotherapy. . Acta Oncologica, 2005. 44: p. 265-276.
[53] Williams, S.G., et al., Use of individual fraction size data from 3756 patients to directly determine the a/b ratio of prostate cancer. . International Journal of Radiation Oncology Biology Physics, 2007. 68(1): p. 24-33.
[54] Garcia, L.M., D.E. Wilkins, and G.P. Raaphorst, a/b ratio: a dose range dependence study. International Journal of Radiation Oncology Biology Physics, 2007. 67(2): p. 587-593.
[55] Koukourakis, M.I., et al., Biological dose volume histograms during conformal hypofractionated accelerated radiotherapy for prostate cancer. Medical Physics, 2007. 34(1): p. 76-80.
[56] Brenner, D.J. and E.J. Hall, Fractionation and protraction for radiotherapy of prostate carcinoma. International Journal of Radiation Oncology Biology Physics, 1999. 43(5): p. 1095-1101.
[57] King, C.R. and C.S. Mayo, Letter to the Editor. Is the prostate a/b ratio of 1.5 from Benner and Hall a modeling artifact? International Journal of Radiation Oncology Biology Physics, 2000. 47(2): p. 536-539.
[58] King, C.R., T.A. DiPetrillo, and D.E. Wazer, Optimal radiotherapy for prostate cancer: predictions for conventional external beam, IMRT, and brachytherapy from radiobiologic models. International Journal of Radiation Oncology Biology Physics, 2000. 46(1): p. 165-172.
[59] Fowler, J., R. Chappell, and M. Ritter, Is a/b for prostate tumors really low? International Journal of Radiation Oncology Biology Physics, 2001. 50(4): p. 1021-1031.
[60] King, C.R. and J.F. Fowler, A simple analytic derivation suggests that prostate cancer alpha/beta ratio is low. International Journal of Radiation Oncology Biology Physics, 2001. 51(1): p. 213-214.
[61] Brenner, D.J., et al., Direct evidence that prostate tumors show high sensitivity to fractionation (low alpha/beta ratio), similar to late-responding normal tissue. International Journal of Radiation Oncology Biology Physics, 2002. 52: p. 6-13.
[62] Wang, J.Z., M. Guerrero, and X.A. Li, How low is the a/b ratio for prostate cancer? . International Journal of Radiation Oncology Biology Physics, 2005. 55: p. 194-203.
[63] Kal, H.B. and M. P. van Gellekom, How low is the alpha/beta ratio for prostate cancer? International Journal of Radiation Oncology Biology Physics, 2003. 57: p. 1116-1121.
[64] Fowler, J.F., Development of radiobiology for oncology - a personal view. Physics in Medicine and Biology, 2006. 51: p. R263-R286.
[65] Nahum, A.E., et al., Incorporating clinical measurements of hypoxia into tumor local control modeling of prostate cancer: Implications for the alpha/beta ratio. International Journal of Radiation Oncology Biology Physics, 2003. 57: p. 391-401.